AIP | Applied Physics Letters

Improved visible light driven photoelectrochemical properties of 3C-SiC semiconductor with Pt nanoparticles for hydrogen generation

Jun Tae Song, Hisanori Mashiko, Masayuki Kamiya, Yoshifumi Nakamine, Akira Ohtomo, Takayuki Iwasaki, and Mutsuko Hatano

Citation: Applied Physics Letters **103**, 213901 (2013); doi: 10.1063/1.4832333
View online: http://dx.doi.org/10.1063/1.4832333
View Table of Contents: http://scitation.aip.org/content/aip/journal/apl/103/21?ver=pdfcov
Published by the AIP Publishing

Improved visible light driven photoelectrochemical properties of 3C-SiC semiconductor with Pt nanoparticles for hydrogen generation

Jun Tae Song,[1] Hisanori Mashiko,[2] Masayuki Kamiya,[1] Yoshifumi Nakamine,[3] Akira Ohtomo,[2] Takayuki Iwasaki,[1] and Mutsuko Hatano[1,a)]
[1]*Department of Physical Electronics, Tokyo Institute of Technology, 2-12-1 Ookayama, Meguro, Tokyo 152-8552, Japan*
[2]*Department of Applied Chemistry, Tokyo Institute of Technology, 2-12-1 Ookayama, Meguro, Tokyo 152-8552, Japan*
[3]*Program for Leading Graduate Schools, Academy for Co-Creative Education of Environment and Energy Science, Tokyo Institute of Technology, 2-12-1 Ookayama, Meguro, Tokyo 152-8552, Japan*

(Received 1 July 2013; accepted 6 November 2013; published online 18 November 2013)

We propose the n-type 3C-SiC with Pt nanoparticles (Pt NPs) as photo-anode for photoelectrochemical hydrogen (H_2) generation. We found that band-edge structure of 3C-SiC is suitable for H_2 generation, and the property can be optimized by dopant (nitrogen) concentration in 3C-SiC. We also confirmed that Pt NPs enhance photoelectrochemical properties showing 0.2%–0.8% higher Incident Photon-to-Current Efficiency than bare 3C-SiC in visible wavelength despite diminished light absorption. Solar-conversion efficiency increases approximately 6.3 times, and H_2 production is improved by 6.5 times with 33% of Faradaic efficiency. Lastly, 3C-SiC surface corrosion is effectively inhibited. © *2013 AIP Publishing LLC*. [http://dx.doi.org/10.1063/1.4832333]

Direct electro-photolysis by electron-hole pairs generated by solar-light in semiconductor materials has been recently attracted as a method for producing hydrogen (H_2) energy from the water. The principle is that solar-light-driven electron-hole pairs in a semiconductor make redox reaction at the interface between the semiconductor surface and aqueous solution, resulting in water-splitting to H_2 and oxygen (O_2). Thus, a semiconductor used as the light-excitation site is important to decide the efficiency of solar-to-hydrogen conversion. Many studies on oxide semiconductor such as TiO_2, WO_3, $BiVO_4$, and ZnO have been reported.[1–6] However, they have drawbacks such as large band-gap, unstability, and unsuitable band-position. These hinder efficient light absorption in the visible light range or cannot be used without hetero-junction for H_2 reduction potential.[7–9] Although GaN has applicable band-structure for the water-splitting, it is necessary to investigate the band-gap engineering for solar spectrum due to its large band-gap (3.4 eV).[10–12]

A SiC semiconductor has a different band-gap according to arrangement of atoms in the structure. 3C (cubic) and 4H (hexagonal) type SiC have a band-gap value of 2.2 and 3.3 eV, respectively. However, there have been few reports on photoelectrochemical (PEC) properties for H_2 generation using SiC photoelectrode.[13–15] 4H-SiC has same limitation as GaN, inefficient for absorbing solar-light due to the large band-gap. Although 3C-SiC has a proper band-gap value of 2.2 eV for solar-light absorption, it suffers from low photo-current and degradation by oxidation.

In this study, we propose the n-type 3C-SiC with Pt nanoparticles (Pt NPs) as photo-anode and achieved the enhancement of PEC properties in the visible light range and long-term stability. Also, the increment of H_2 gas production by Pt NPs is reported.

Figure 1 shows the basic principle for direct electro-photolysis by solar-light energy and PEC cell with a quartz window utilized to reduce the loss of incident light. The free-standing n-type 3C-SiC wafers (with a lightly (1.0×10^{16} cm^{-3}) and highly (3.6×10^{18} cm^{-3}) nitrogen concentration) were obtained by low pressure chemical vapor deposition (LPCVD) on the Si substrate and then eliminating Si substrate. Here, nitrogen is the dopant for 3C-SiC. The aluminum (Al) layer 2 μm in thickness was deposited by sputtering on the backside of the SiC wafers for Ohmic contact. Then, the copper wire was connected on the Al layer, and the back and sides of the SiC sample piece were covered by the adhesive for insulation. As for the formation of the Pt NPs, a Pt layer ~2 nm in thickness was deposited by sputtering on the bare 3C-SiC surface. The sample was annealed at 400 °C for 30 min under Ar atmosphere to form particles. The particle formation was confirmed by atomic force microscope (AFM). As a counter and a reference electrode, Pt and Ag/AgCl were used, respectively. Then, these three electrodes were immersed in 0.01M HCl (pH = 1.12) aqueous solution. A solar-light lamp (USHIO Optical ModuleX) with a variable power density was used as a light source. Impedance and voltammetry measurements were implemented by Potentiostat (Princeton Applied Research VersaSTAT 3). The impedance of the photo-anode was measured in the frequency range from 0.1 Hz to 20 kHz. Photo-currents were measured by linearly sweeping the applied bias from −0.1 to 1.5 V (vs. Ag/AgCl) at a scan rate of 50 mV/s. The amount of evolved H_2 gas after PEC reaction was analyzed by gas chromatography (Inficon Micro GC 3000) using Ar carrier gas. Moreover, we obtained single-wavelength by monochromator with Xe light source for Incident Photon-to-Current Efficiency (IPCE) and used UV-Vis spectrometer (Shimazu UV-3150) for absorption spectrum.

First, we investigated basic properties of 3C-SiC photo-anode for H_2 generation by PEC reaction with solar-light

a)Electronic mail: hatano.m.ab@m.titech.ac.jp

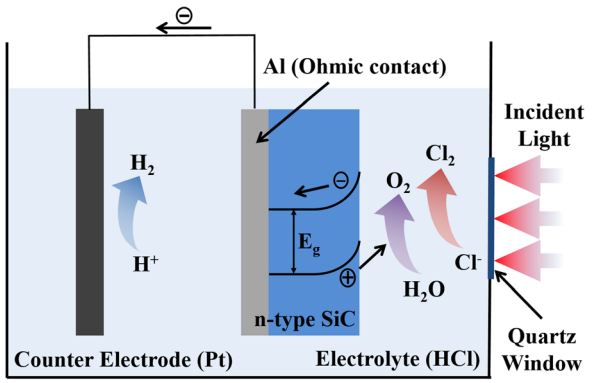

FIG. 1. Schematic illustration of the PEC cell. Generated carriers by solar-light in the photo-anode move to surfaces on the working (3C-SiC) and counter electrodes, and then redox reactions occur. In this experiment, Cl^- ions from HCl electrolyte are also oxidized to Cl_2 at working electrode side.

energy. Fig. 2(a) shows a Mott-Schottky plot for n-type 3C-SiC obtained by impedance measurement from −2.6 V to −0.7 V in the electrolytes of pH 1.12, 8.36, and 12.84. We applied the equivalent circuit which consists of the series resistance (R_s), depletion region resistance (R_p), and capacitance (C) at the interface as shown in Fig. 2(a). The intercept points of linear fitted lines and x-axis correspond to flat-band potential, V_{fb}, −1.1 V, −1.15 V, and −1.4 V for pH 1.12, 8.36, and 12.84, respectively. The band-edge potential can be obtained by measured V_{fb} as shown in Fig. 2(b) with pH.[16] Conduction band-edge is more negative than hydrogen-evolving potential (H_2/H^+), and valence band-edge is more positive than oxygen-evolving potential (H_2O/O_2). This result means that 3C-SiC photo-anode is basically applicable for direct electro-photolysis to generate H_2 by only solar-light. Fig. 2(c) shows linear sweep voltammetry of highly and lightly doped 3C-SiC for photo-response. In the inset of Fig. 2(c), it is shown that the highly and lightly doped electrodes have photo-current densities of 4 and 7 $\mu A/cm^2$ without applied bias (0 V). Photo-current densities increase to 0.13 and 0.20 mA/cm^2 from the highly and lightly doped samples at an applied bias of 1 V, respectively. The photo-current density for the lightly doped sample is higher than that of highly doped one. Also, the lightly doped 3C-SiC has the onset potential, which is the intercept of potential axis and the fitted line for linear part of the curve, ~1.2 V lower than ~1.3 V for the highly doped. The width of depletion layer formed at the interface between photo-anode and electrolyte becomes broader, and the life-time for the light-generated minority carrier, holes, is longer, as the doping density of the 3C-SiC is smaller. Therefore photo-current density increased in case of the lightly doped 3C-SiC. The solar-conversion efficiency (η) at an applied bias is also estimated by using the followed equation:[17]

$$\eta = \frac{i(1.23 - E)}{P_{in}A} \times 100, \quad (1)$$

where i (A) is a photo-current obtained after stabilizing photo-current with time at an applied bias, E (V) converted to reversible hydrogen electrode (RHE) scale via Nernst equation from measured potential vs. Ag/AgCl for pH independence. 1.23 is the minimum potential (V) for the water-splitting, P_{in} (W/cm^2) is the power density of incident light

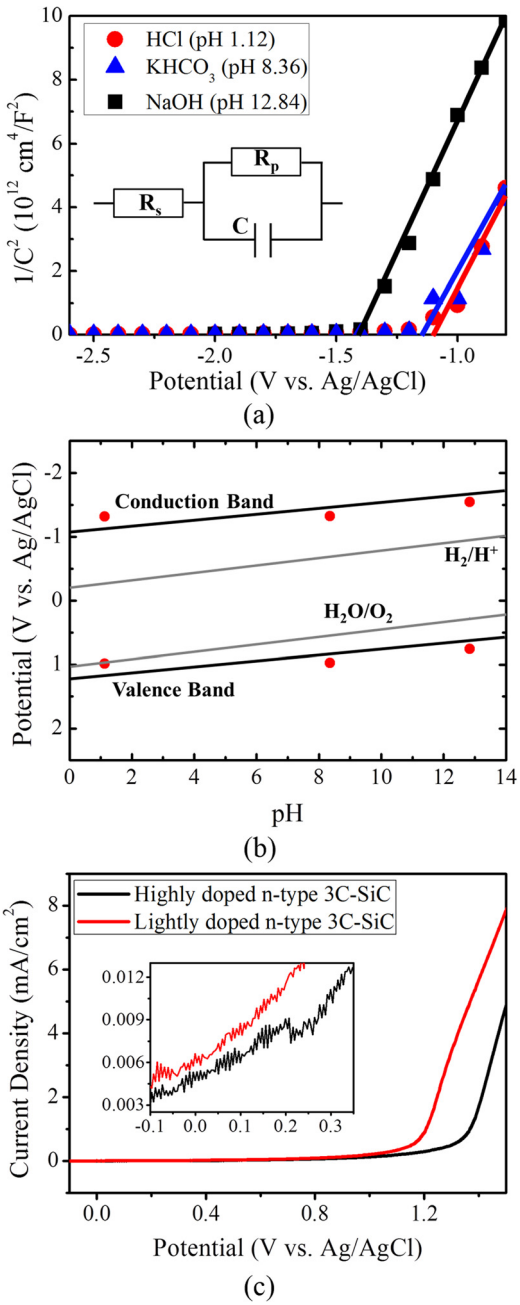

FIG. 2. (a) Mott-Schottky plots for n-type 3C-SiC obtained from an impedance measurement in different electrolytes. The linearly fitted line is drawn to calculate flat-band potential (V_{fb}) (intercepts at x-axis). The applied equivalent circuit is expressed inside the graph. (b) n-type 3C-SiC band-edge position as a function of pH (0.01M HCl (pH 1.12), 0.1M $KHCO_3$ (pH 8.36), and 0.1M NaOH (pH 12.84)). (c) Photo-current density vs. potential for highly and lightly nitrogen-doped 3C-SiC under light illumination. The inset is the magnified graph in the range from −0.1 V to 0.35 V. The applied power density of lamp is 994 mW/cm^2.

source, and A (cm^2) is the working electrode surface area. The efficiency at an applied bias of 1 V (vs. RHE) for lightly doped 3C-SiC efficiency is calculated approximately to 2 times higher than highly doped 3C-SiC sample. Although 3C-SiC photo-anode has proper conditions for H_2 generation, another reason such as stacking faults in SiC, which shorten the carrier life time, cause the low efficiency.

In order to enhance the efficiency of 3C-SiC photo-anode, we formed Pt NPs on the surface of bare 3C-SiC. Even though 3C-SiC satisfies proper band-gap value for

visible light absorption, it shows insufficient solar-conversion efficiency. Here, Pt is a very chemically stable material and expected to be proper co-catalyst which improves transfer of holes from an anode to an electrolyte due to the band-bending at interface between SiC and Pt. Pt NPs with a size of ~3 nm were formed as shown in the inset of Fig. 3. Figure 3 shows the linear sweep voltammetry of bare 3C-SiC (lightly ($1.0 \times 10^{16}\,cm^{-3}$) nitrogen-doped) and Pt NPs/3C-SiC. In the case of Pt NPs/3C-SiC, the photo-current density dramatically increases to 2.03 mA/cm^2 at an applied bias of 1 V while it is 0.14 mA/cm^2 for bare 3C-SiC. The onset potential is also shifted to ~0.7 V, lower than ~1.2 V without the Pt NPs. As a result, the solar-conversion efficiency at an applied bias of 1 V (vs. RHE) becomes about 6.3 times greater than bare 3C-SiC.

Figure 4 shows the results of H_2 gas production amount after PEC reaction with bare 3C-SiC and Pt NPs/3C-SiC photo-anode. Produced H_2 gas was collected after PEC reaction for 10 min at an applied bias of 1 V (vs. Ag/AgCl) with varying incident light power density, separately. The H_2 gas production amount increases linearly with elevation of the light power density for both bare 3C-SiC and Pt NPs/3C-SiC proving that the H_2 generation occurs by the PEC reaction. Apparently, the amount of H_2 generation for Pt NPs/3C-SiC is larger than bare 3C-SiC. Under the incident light with power density of 492 and 628 mW/cm^2, we obtained about 6.5 times higher H_2 gases for Pt NPs/3C-SiC. It almost corresponds to increase rate of photo-currents, 6.3 times by Pt NPs. The difference should mostly come from negligible measurement errors. Even at a lower power density of 355 mW/cm^2, Pt NPs/3C-SiC shows assurable H_2 generation, 2.4 μmol/cm^2, while bare 3C-SiC produces little amount of H_2 gas. In addition, Faradaic efficiency of H_2 generation is also improved by Pt NPs from 29.5% to about 33%. Therefore, it is clearly demonstrated that Pt NPs contributes improvement of PEC properties for H_2 production.

We investigated UV-Vis absorption and IPCE to clarify the reason of improved efficiency by Pt NPs as shown in Fig. 5. It is confirmed that 3C-SiC can absorb the light with wavelength shorter than 545 nm corresponding to energy, 2.28 eV, which is almost same with the band-gap (2.2 eV) as

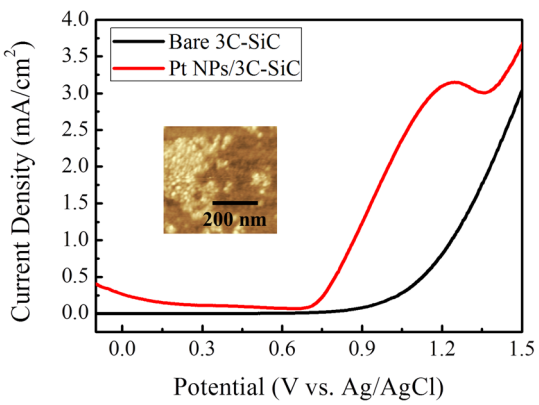

FIG. 3. Photo-current density vs. potential for comparing bare 3C-SiC (lightly ($1.0 \times 10^{16}\,cm^{-3}$) nitrogen-doped sample) and Pt NPs/3C-SiC. Pt NPs/3C-SiC shows the enhanced photo-current density and the lower onset potential. The inset is the AFM image for the surface of the sample which has Pt NPs with size of ~3 nm.

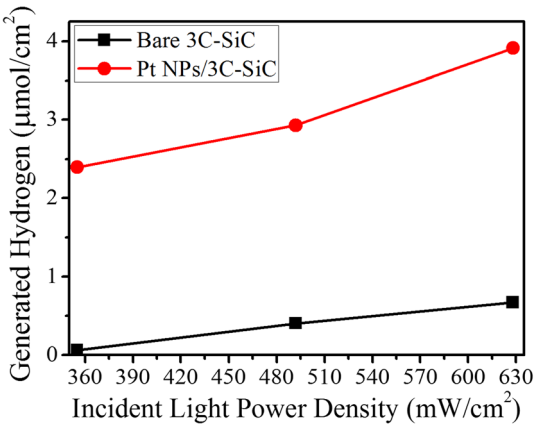

FIG. 4. Hydrogen production amount generated at counter electrode in accordance with incident light power density. Incident light power density is 355, 492, and 628 mW/cm^2.

shown in Fig. 5(a). That is, the range below 545 nm is considered as effective range for light absorption. Although UV-Vis absorption for Pt NPs/3C-SiC is higher than bare 3C-SiC above the 503 nm, UV-Vis absorption of Pt NPs/3C-SiC becomes lower than bare 3C-SiC in wavelength shorter than 503 nm in the effective range. It means the improvement of PEC property by Pt NPs is not caused by absorption effect.

Next, we show the IPCE results as shown in Fig. 5(b). The photo-current for IPCE was collected under 1 V (vs. Ag/AgCl) bias. IPCE can be expressed as

$$\mathrm{IPCE}(\lambda) = \frac{|j_{ph}(\mathrm{mA/cm^2})| \times 1239.8(\mathrm{V \times nm})}{\mathrm{P_{mono}(mW/cm^2)} \times \lambda(\mathrm{nm})}, \qquad (2)$$

where P_{mono} and λ are power density and the wavelength of the monochromated incident light, respectively, j_{ph} is the photo-current density, and 1239.8 is the multiplication of h (Planck's constant) and c (velocity of light). While UV-Vis

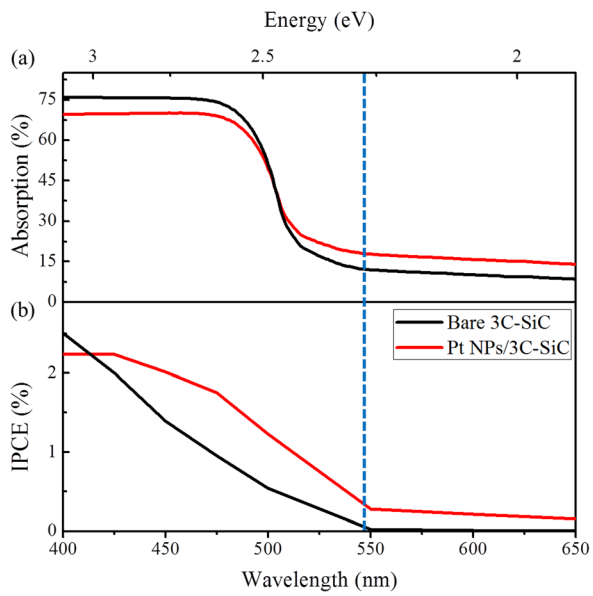

FIG. 5. Comparison of UV-Vis absorption (a) and IPCE (b) spectra for bare 3C-SiC and Pt NPs/3C-SiC. Photo-current was measured at 1 V (vs. Ag/AgCl) bias for IPCE. Blue dotted line indicates the threshold energy for band-gap transition, 545 nm (2.28 eV).

absorption for Pt NPs/3C-SiC is lower than bare 3C-SiC, Pt NPs/3C-SiC shows 0.2%–0.8% higher IPCE in the range of wavelength of 412–550 nm. The integration of the spectrum for Pt NPs/3C-SiC in 400–550 nm is ~40% larger than that of bare 3C-SiC, indicating that contribution to much higher efficiency in visible range. Consequently, the enhanced PEC property is caused by not absorption effect but improved carrier transport due to band-bending between 3C-SiC and Pt NPs. Also, the higher IPCE by Pt NPs in visible light range means that Pt NPs/3C-SiC should more efficiently use the spectrum of solar-light lamp which contains 40% visible light in the range of 200–800 nm. Namely, Pt NPs hinder the photon absorption but contribute to improve the PEC reaction in the visible range.

Lastly, the time-dependent measurements under light illumination were performed for about 5 h in order to investigate the stability of bare 3C-SiC and Pt NPs/3C-SiC sample. It is known that SiC is dissolved by oxidation reaction, and SiO_2 is formed on the surface from the following reaction:[18,19]

$$2SiC + 6H_2O + 12h^+ = SiO_2 + CO_2 + SiO + CO + 12H^+. \quad (3)$$

In this measurement, bare 3C-SiC and Pt NPs/3C-SiC samples were applied by 1.3 V and 1 V (vs. Ag/AgCl), respectively, for comparing two samples in similar electric charge quantity. The result of time-dependent measurement is shown in Fig. 6. The total quantity of electric charge after 5 h for the bare 3C-SiC is 7 C, same with total quantity after 2.4 h for Pt NPs/3C-SiC sample. In spite of lower electric charge flow for bare 3C-SiC, photo-current densities without Pt NPs after reaction for about 5 h decrease by 93% much higher than 65%, which is decrease rate for Pt NPs/3C-SiC. The photo-current finally decreases to 0.5 and 0.1 mA/cm^2 with and without the Pt NPs, respectively. Due to the preferential oxidation reaction at the Pt NPs surface, the degradation is effectively suppressed.

In summary, we demonstrated that the n-type 3C-SiC has proper band-structure (position and band-gap) for H_2 generation by solar-light. Lightly doped 3C-SiC shows higher solar-conversion efficiency than highly doped sample, suggesting photo-current can be optimized by nitrogen doping density. In order to enhance the performance of 3C-SiC photo-anode, it is found that Pt NPs as co-catalyst on 3C-SiC surface is attributed to improve carrier transport and stability. Although absorption becomes lower with Pt NPs, IPCE is improved in the visible light range. Therefore, the solar-conversion efficiency is enhanced by 6.3 times with Pt NPs. Accordingly, H_2 gas generation amount by Pt NPs is grown by about 6.5 times with improved Faradaic efficiency from 29.5% to 33%. Furthermore, Pt NPs effectively inhibit degradation of 3C-SiC. The Pt NPs suggest significant advantages for visible light driven PEC reaction for H_2 generation on 3C-SiC photo-anode considered as the most suitable material in many poly-types of SiC.

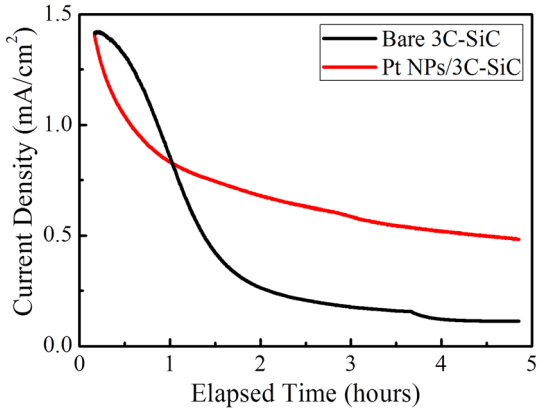

FIG. 6. Photo-current density vs. elapsed time for the stability examination of 3C-SiC photo-anode. In order to neglect irrelevant initial reaction, photo-currents after 10 min are considered in this graph.

We deeply thank "Yazaki memorial foundation for science & technology and the Mazda Foundation" for the support of this research.

[1]W. Siripala, A. Ivanovskaya, T. F. Jaramillo, S. Baeck, and E. W. McFarland, Sol. Energy. Mater. Sol. Cells **77**, 229 (2003).
[2]J. H. Park, S. Kim, and A. J. Bard, Nano Lett. **6**, 24 (2006).
[3]A. Fujishima and K. Honda, Nature **238**, 37 (1972).
[4]S. J. Hong, S. Lee, J. S. Jang, and J. S. Lee, Energy Environ. Sci. **4**, 1781 (2011).
[5]K. Sayama, A. Nomura, T. Arai, T. Sugita, R. Abe, M. Yanagida, T. Oi, Y. Iwasaki, Y. Abe, and H. Sugihara, J. Phys. Chem. B **110**, 11352 (2006).
[6]M. A. Butler, J. Appl. Phys. **48**, 1914 (1977).
[7]C. X. Kronawitter, L. Vayssiers, S. Shen, L. Guo, D. A. Wheeler, J. Z. Zhang, B. R. Antoun, and S. S. Mao, Energy Environ. Sci. **4**, 3889 (2011).
[8]R. Saito, Y. Miseki, and K. Sayama, Chem. Commun. **48**, 3833 (2012).
[9]Y. J. Hwang, A. Boukai, and P. Yang, Nano Lett. **9**, 410 (2009).
[10]K. Fujii, T. Karasawa, and K. Ohkawa, Jpn. J. Appl. Phys., Part 2 **44**, L543 (2005).
[11]S. Yotsuhashi, M. Deguchi, H. Hashiba, Y. Zenitani, R. Hinogami, Y. Yamada, and K. Ohkawa, Appl. Phys. Lett. **100**, 243904 (2012).
[12]T. Hayashi, M. Deura, and K. Ohkawa, Jpn. J. Appl. Phys., Part 1 **51**, 112601 (2012).
[13]J. Akikusa and S. U. M. Khan, Int. J. Hydrogen Energy **27**, 863 (2002).
[14]Q. Ma, B. Kaiser, J. Ziegler, D. Fertig, and W. Jaegermann, J. Phys. D: Appl. Phys. **45**, 325101 (2012).
[15]T. Yasuda, M. Kato, M. Ichimura, and T. Hatayama, Appl. Phys. Lett. **101**, 053902 (2012).
[16]J. D. Bach, R. T. Collins, and J. A. Turner, J. Electrochem. Soc. **150**, A899 (2003).
[17]S. U. M. Khan, M. Al-Shahry, and W. B. Ingler, Science **297**, 2243 (2002).
[18]M. Kato, M. Ichimura, and E. Arai, Jpn. J. Appl. Phys., Part 1 **40**, 1145 (2001).
[19]J. S. Shor and A. D. Kurtz, J. Electrochem. Soc. **141**, 778 (1994).